Cell

A Dual Program for Translation Regulation in Cellular Proliferation and Differentiation

Hila Gingold,[1,15] Disa Tehler,[2,15] Nanna R. Christoffersen,[2] Morten M. Nielsen,[5] Fazila Asmar,[9] Susanne M. Kooistra,[2] Nicolaj S. Christophersen,[2] Lise Lotte Christensen,[5] Michael Borre,[6] Karina D. Sørensen,[5] Lars D. Andersen,[5] Claus L. Andersen,[5,7] Esther Hulleman,[11] Tom Wurdinger,[12,13] Elisabeth Ralfkiær,[10] Kristian Helin,[2,3,4] Kirsten Grønbæk,[9] Torben Ørntoft,[5] Sebastian M. Waszak,[14] Orna Dahan,[1] Jakob Skou Pedersen,[5,8] Anders H. Lund,[2,*] and Yitzhak Pilpel[1,*]
[1]Department of Molecular Genetics, The Weizmann Institute of Science, Rehovot 76100, Israel
[2]Biotech Research and Innovation Centre
[3]Center for Epigenetics
[4]The Danish Stem Cell Center (Danstem)
University of Copenhagen, 2200 Copenhagen, Denmark
[5]Department for Molecular Medicine
[6]Department of Urology
[7]Department of Surgery
[8]Bioinformatics Research Centre
Aarhus University Hospital, 8000 Aarhus, Denmark
[9]Department of Hematology
[10]Department of Pathology
Rigshospitalet, University of Copenhagen, 2100 Copenhagen, Denmark
[11]Department of Pediatric Oncology
[12]Department of Neurosurgery
Neuro-oncology Research Group, Cancer Center Amsterdam, VU University Medical Center, 1007 MB Amsterdam, the Netherlands
[13]Department of Neurology, Massachusetts General Hospital and Harvard Medical School, Boston, MA 02114, USA
[14]Institute of Bioengineering, School of Life Sciences, École Polytechnique Fédérale de Lausanne, 1015 Lausanne, Switzerland
[15]Co-first author
*Correspondence: anders.lund@bric.ku.dk (A.H.L.), pilpel@weizmann.ac.il (Y.P.)
http://dx.doi.org/10.1016/j.cell.2014.08.011

SUMMARY

A dichotomous choice for metazoan cells is between proliferation and differentiation. Measuring tRNA pools in various cell types, we found two distinct subsets, one that is induced in proliferating cells, and repressed otherwise, and another with the opposite signature. Correspondingly, we found that genes serving cell-autonomous functions and genes involved in multicellularity obey distinct codon usage. Proliferation-induced and differentiation-induced tRNAs often carry anticodons that correspond to the codons enriched among the cell-autonomous and the multicellularity genes, respectively. Because mRNAs of cell-autonomous genes are induced in proliferation and cancer in particular, the concomitant induction of their codon-enriched tRNAs suggests coordination between transcription and translation. Histone modifications indeed change similarly in the vicinity of cell-autonomous genes and their corresponding tRNAs, and in multicellularity genes and their tRNAs, suggesting the existence of transcriptional programs coordinating tRNA supply and demand. Hence, we describe the existence of two distinct translation programs that operate during proliferation and differentiation.

INTRODUCTION

An important dichotomy in the life of a cell in many multicellular species is between proliferation and differentiation. The classic *The Hallmarks of Cancer* (Hanahan and Weinberg, 2000) states that "…cells may be induced to permanently relinquish their proliferative potential by being induced to enter into postmitotic states, usually associated with acquisition of specific differentiation-associated traits." Indeed, proliferation and differentiation are often distinct cellular states; generally, differentiated cells are less proliferative, and proliferating cells are typically not terminally differentiated. Cancer demonstrates this dichotomy, as transformed cells sometimes lose their original differentiation marks (Kumar et al., 2012). This dichotomy was also illustrated in normal liver (Klochendler et al., 2012), in which a small percentage of proliferative cells show reduced levels of liver differentiation markers.

So far, most studies that examined gene-expression programs in proliferation, cancerous in particular, and differentiation focused on the *transcriptome* (Dutkowski and Ideker, 2011; Perou et al., 2000). More recently, interest increased in measuring *translation* and its changes in cancer (Hsieh et al., 2012; Pavon-Eternod et al., 2009) and in differentiating cells (Ingolia

et al., 2011). Originally, the interest in translation was mainly focused on initiation (Mamane et al., 2006; Sonenberg and Hinnebusch, 2009), yet, more recently, attention toward elongation has increased (Hsieh et al., 2012). The secondary structure of the mRNA was recognized as a prime factor affecting initiation and early elongation (Goodman et al., 2013; Kudla et al., 2009; Tuller et al., 2010). However, whether this essential attribute of mRNAs can be programmed to change dynamically across conditions is unknown. The cellular tRNA pool is another prime factor that controls translation (reviewed in Gingold and Pilpel, 2011; Subramaniam et al., 2013; Tuller et al., 2010), and a role of the tRNA pool in cancer and across differentiated tissues is beginning to be characterized. Small-RNA sequencing (Yang et al., 2010) and tRNA customized arrays (Pavon-Eternod et al., 2009) have provided data regarding changes in tRNA availability in cancer. Occupancy of the tRNA polymerase, RNA Pol III, in the vicinity of tRNA genes was measured across organs and species (Kutter et al., 2011; Raha et al., 2010) as were the histone epigenetic marks in their vicinity (Barski et al., 2010; Oler et al., 2010). Yet, it remains unknown which tRNAs display which types of changes in various cell types and how they affect and are affected by the transcriptome and by cellular physiology.

If we consider the tRNA as the "supply" in translation, then the codon usage in the transcriptome is the "demand" (reviewed in Gingold and Pilpel, 2011). The balance between supply and demand, i.e., the extent of adaptation of the tRNA pool to the codon usage in the transcriptome, could affect production levels of proteins (Qian et al., 2012). In addition, cellular fitness could be affected by the extent of a global codon-to-tRNA adaptation (Kudla et al., 2009; Navon and Pilpel, 2011), and especially highly expressed genes appear to be codon optimized (Gingold et al., 2012). It was suggested that low compatibility between demand and supply, especially if presented by highly expressed genes, can result in a global inefficient allocation of resources such as ribosomes and thus could be fitness reducing (Kudla et al., 2009). Hence, production costs and production throughput are prime factors that can be influenced by coordination between tRNA supply and demand. Equally interesting are cases in which certain genes appear to be selected for deliberately low codon-to-tRNA adaptation, e.g., as in the case of some circadian clock genes (Xu et al., 2013; Zhou et al., 2013).

Here we measured the tRNA pool in hundreds of proliferating and differentiating samples, including cancers and normal cells. We found that the tRNAs that are induced in proliferating cells are typically repressed in differentiating/arresting cells, and that they carry anticodons which often correspond to a codon usage signature that is characteristic of proliferation-related genes. Conversely, the tRNAs that are induced in differentiating cells are often found to be repressed in proliferating cells and to be better tuned to a characteristic codon-usage preference of the differentiation-related genes.

RESULTS

Opposing tRNA Signatures in Proliferation and Differentiation

In order to follow changes in the tRNA pool in a diversity of proliferating, differentiating/differentiated, and arrested cells, we used two complementary experimental platforms: microarrays and the histone modification maps in the genomic vicinity of the tRNA genes. First, we designed and printed microarrays that probe human tRNAs (in addition to other noncoding and coding genes). Our array platform represents tRNAs for most amino acids and anticodon types, excluding tRNAs that are either prone to cross-hybridization or that have low tRNA scores (Lowe and Eddy, 1997) (see Experimental Procedures, Extended Experimental Procedures, and Table S3). We used the arrays to measure expression levels of tRNAs in 470 samples that represent various states of proliferation (normal or cancerous), differentiation or growth arrest, and senescence (see Table 1). Our proliferating cells consisted of both primary tumors and cancer cell lines from diffuse large B cell lymphoma (DLBCL), bladder, colon, glioblastoma, and prostate cancer. In addition, we also examined immortalized normal fibroblasts that were induced to proliferate by expression of key oncogenes, or after release from serum starvation. Our differentiated cells included normal cells from each of the above tumor sources, in addition to embryonic stem cells (ESCs) after induction of differentiation. In addition, we inspected immortalized fibroblast cells at two arrested conditions, namely after induction of senescence and in response to serum starvation. In parallel to the microarrays, we analyzed ENCODE data sets (Bernstein et al., 2012) and additional sources (Bert et al., 2013; Gifford et al., 2013). We inspected the vicinity of the human tRNA genes with respect to several histone modifications that are associated with either active transcription or repression, in addition to examining occupancy by RNA Pol III (Oler et al., 2010).

The two experimental platforms are complementary, examining the expression of the tRNAs themselves and their genomic regions and transcriptional statuses, respectively. Reassuringly, the tRNA abundance measurements obtained with the arrays correlate well (Pearson coefficient = 0.54 to 0.71 for the various conditions) with transcription activation-associated chromatin modifications as measured in ENCODE across all represented tRNAs (Figure 1A). We first focused on the expression measurements based on microarray platform.

Figure 1B shows the relative changes in the tRNA pool in each of 68 patients with DLBCL compared to the tRNA levels in normal B cells from ten healthy donors. Overall, the tRNA pool changes reproducibly among the lymphoma patients, e.g., the median Pearson correlation among all pairs of samples was 0.66. Whereas the expression of some tRNA genes is elevated more than 10-fold in cancer, the expression of others decreases more than 10-fold. Interestingly, in some cases, tRNAs that translate different codons for the same amino acid show opposite trends.

Comparing the tRNA pool changes in several cancer types, each relative to its corresponding normal tissue, we found a high similarity among the patients within each given cancer type (Figure 1C, values on the diagonal), and also a significant, albeit lower, similarity between different cancers (Figure 1C, off-diagonal).

Cancerous samples, and even cancer cell lines, are complex and can be heterogeneous. To complement the picture that emerges from such samples, and to examine whether the proliferation/differentiation statuses of cells are reflected in their tRNA pools, we established a series of manipulated noncancerous

Table 1. Overview of Samples Used for RNA Expression Profiling

Cancer/Model System	Samples/Cell Lines	Sample Description/Experiment
Primary Cancers		
Bladder cancer	patient samples and cancer cell lines	tumor samples (n = 83), normal tissue (n = 8), bladder cancer cell lines (n = 13)
Colon cancer	patient samples and cancer cell lines	carcinoma samples (n = 44), adenoma samples (n = 39), adjacent normal mucosa (n = 16), colon cancer cell lines (n = 10)
Diffuse large B cell lymphoma	patient samples and cancer cell lines	tumor samples (n = 68), normal B cells (n = 10), DLBCL cell lines (n = 2)
Glioblastoma	patient samples and cancer cell lines	tumor samples (n = 71), normal brain (n = 2), glioblastoma cell lines (n =2)
Prostate cancer	patient samples and cancer cell lines	tumor samples (n = 28), normal tissue (n = 11), prostate cancer cell lines (n = 3)
Model Systems		
Differentiation	human embryonic stem cells (hESC)	ATRA-induced differentiation of hESCs after 0, 1, 3, and 5 days (n = 3 per time point)
Serum starvation	human fibroblast cells: BJ/hTERT	proliferating and serum-starved human fibroblast cells with re-introduction of serum for 30 min, 2 hr, and 4 hr (n = 3 per time point)
Senescence	human fibroblast cells: TIG3/hTERT/BRAF::ER	BRAF-induced senescence versus control in human fibroblast cells after 4 hr and 72 hr (n = 3 per time point)
MYC overexpression	human fibroblast cells: BJ/hTERT	human fibroblast cells with overexpression of MYC or control vectors for 24 hr and 72 hr (n = 3 per time point)
RAS overexpression	human fibroblast cells: BJ/hTERT	human fibroblast cells with overexpression of HRASV12 or control vectors for 24 hr and 72 hr (n = 3 per time point)

cells that were induced either to proliferate, to arrest growth, to senesce, or to differentiate.

We first examined the tRNA pool in normal human fibroblasts induced to proliferate by a 4 hr time course of serum stimulation following a period of serum starvation-induced cell-cycle arrest. In addition, we examined the same cell type 72 hr after overexpression of either of the oncogenes MYC or HRASV12. The model systems were validated for oncogene overexpression and induction of relevant proliferation and differentiation markers (Figures S1A and S1B). We found that the tRNA pool changes similarly among all proliferating samples, either cancerous or noncancerous (Figure 1C).

To determine the tRNA profile in differentiated and arresting cells, we created three different model systems: (1) human ESCs (hESCs) induced to differentiate with retinoic acid; (2) BRAF-induced senescence in human fibroblasts; (3) induced cell-cycle arrest in human fibroblasts by serum starvation. Here too we validated that the treatments yielded the expected response (Figures S1C and S1D). The changes in tRNA levels were typically positively correlated among all the differentiated and arrested cells, whereas they were overall negatively correlated with the changes observed in the proliferating samples (Figure 1C). Figure 1D illustrates a collection of correlation plots between the tRNA pool changes among the proliferative samples ($0.38 < \text{Spearman's rho} < 0.69$; all p values < 0.05), as well as the negative correlations between proliferative and differentiating/arresting samples ($-0.7 < \text{Spearman's rho} < -0.42$; all p values < 0.05).

Two special tRNAs, the initiator methionine and the selenocysteine, are noticeable (Figure S1E). The initiator methionine tRNA, but not the elongator, is induced in most proliferating samples and repressed in the differentiating or arresting cells. These results are in line with a study showing that overexpression of the initiator tRNA-Met elevates cell proliferation in human epithelial cells (Pavon-Eternod et al., 2013). Conversely, the tRNA for selenocysteine is repressed in many of the proliferating cells and in cancers in particular, in line with a known anticancerous effect of selenocysteine (Almondes et al., 2010).

Next we used principal-component analysis (PCA) to represent the similarity between the tRNA pools at all time points in these model systems. In this representation, each time point in each treatment is represented by a dot, pairs of samples with similar tRNA dynamics are adjacent on the plane, and arrows represent the direction of time in each treatment. Interestingly, we obtained a continuous spectrum, on one side of which are the tRNA pools of the differentiated, senescent, and arrested cells, and at the other extreme are the proliferating, starvation-released cells (Figure 1E). Following the tRNA pools along each process, we observed a gradual smooth transition to one of the two extremes: cells induced for differentiation or senescence gradually change their tRNA pool oppositely from proliferating cells.

Importantly, the similarity of the tRNA pools among the proliferative samples, and conversely among the differentiated/arrested samples, does not reflect a global transcriptome-wide pattern. When we instead clustered the various samples based on mRNA expression changes, we found a markedly different picture in which samples are clustered together according to their tissue origin rather than by proliferation/differentiation status (Figure S1F). These results indicate that whereas the mRNA expression captures a tissue identity signature, the tRNA pool mainly reflects information about proliferative status of the cell.

This conclusion also holds true when examining the tRNA pools using a completely different experimental platform, i.e., the epigenetic status of tRNA genes in the genome. We analyzed the ENCODE data set (Bernstein et al., 2012) and checked the vicinity of tRNA genes with respect to histone modifications

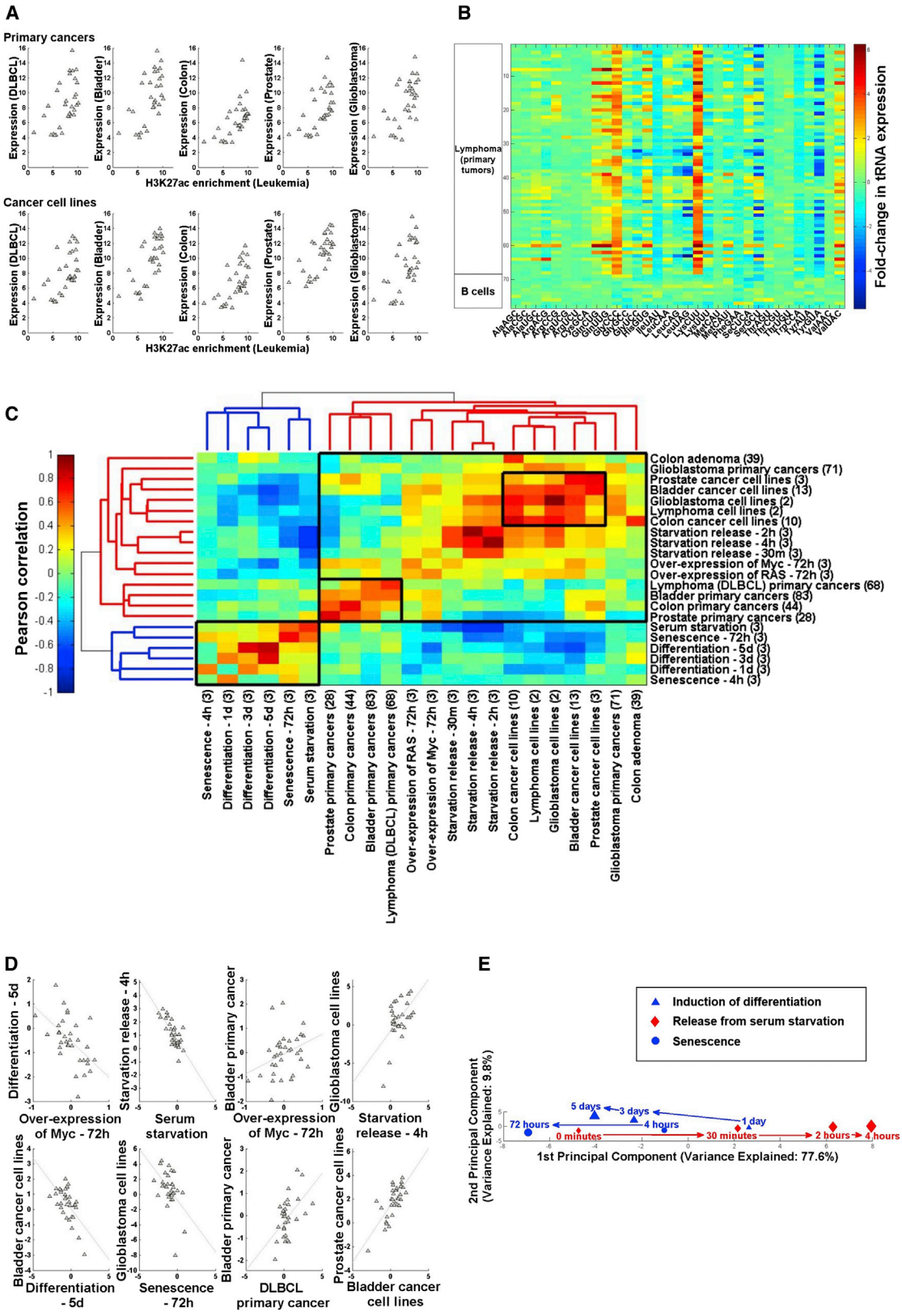

(legend on next page)

associated with active or repressed transcription, which were shown to function similarly at Pol III genes and Pol II transcriptional units (Barski et al., 2010; Oler et al., 2010). We found a similar trend as observed in the arrays: the transcriptional activity status in the vicinity of the tRNA pool is similar in differentiated cells, however it takes a distinct form in cancer cells (Figure S1G).

A Distinct Codon-Usage Signature of Proliferation-Related Genes and Genes Involved in Differentiation and Multicellularity

If each tRNA was equally required for translation of genes involved in proliferation and differentiation, then any increase or decrease in the expression of a given tRNA would have affected the translation of all genes in a similar direction. Under this assumption, it would be unclear why certain tRNAs increase, whereas others decrease in expression during proliferation or differentiation. We thus hypothesized that the differential regulation of the tRNAs might be rooted in a distinction in codon usage of genes involved in proliferative or differentiation processes. To examine this possibility, we analyzed codon usage in genes belonging to various functional categories. We first focused on two functional gene sets of the Gene Ontology (GO) classification (Ashburner et al., 2000), namely the "M phase of mitotic cell cycle" (92 genes) and "pattern specification" (82 genes), i.e., genes involved in differentiation. We computed codon usage for each of the 61 codons for the genes in each of the two categories (correcting for potential amino acid usage biases, see Figure 2A legend) and observed a remarkable dichotomy: for most amino acids, there exists at least one codon that is preferentially used in the cell-cycle genes and at least one distinct codon that is preferentially used in the pattern-specification genes (Figure 2A and Table S1). Interestingly, the cell-cycle-preferred codons tend to have an A or a T nucleotide at the 3rd codon position, whereas the pattern-specification preferred codons have a tendency to end with G or C nucleotides (Figure S2A). Although it is generally the case that cell-cycle-related genes are more AT rich, it is particularly their 3rd nucleotide codon position that is more AT rich (Figure S2A). Notwithstanding, it is well known that promoters of cell-autonomous/housekeeping genes reside in CpG islands (Saxonov et al., 2006), thus the high A/T content of the cell-cycle genes in the 3rd codon position appears to be a distinct phenomenon. Interestingly, whereas the cell-autonomous functions are characterized by high CpG content in their promoters, multicellularity functions that are not related to development and patterning are characterized by low CpG promoter content (Figure S2B).

Examining all major GO categories in human, including all "Biological Process" categories that include at least 40 genes, we calculated for each the average codon usage of its constituent genes. We used PCA to visualize similarity in codon usage between all gene sets (Figure 2B). In this display, two gene sets are close if they have a similar codon-usage pattern and are far apart otherwise. The above-mentioned sets "M phase of mitotic cell cycle" and "pattern specification" are at the two "poles" of the projection, thus representing the two most distinct gene sets in terms of codon usage. Interestingly, the first three PCs alone span >70% of the variance of the data. A striking result was that especially along the first PC, there is a clear separation between gene categories related to development and multicellularity processes on one side and genes related to cellular proliferation and other cell-autonomous processes on the other (Figure 2B). Particularly, at one end of the first PC axis, we found genes involved in processes such as cell cycle, DNA replication and cell division, transcription, translation, mRNA metabolic process, mRNA splicing, DNA repair, protein folding, and nucleosome assembly. In contrast, on the other side of the plane, we found functionalities related to differentiation and developmental patterning in addition to other multicellularity processes such as cell adhesion, cell-junction assembly, toll-like receptor signaling, and extracellular matrix. We also examined the GO category "negative regulation of cell cycle" and found these genes to reside away from their respected regulated cell-cycle genes targets. Likewise, angiogenesis genes reside closer to the "multicellular" side, yet "negative regulators of angiogenesis" have a more proliferation-like codon usage. These findings show how network properties, such as sign of a regulatory effect, can be encoded in the codon selection of genes.

Interestingly, whereas the first PC separates GO functional gene sets according to the cell-autonomous versus multicellularity functionalities, the second PC separates, although much more modestly, the development and embryonic patterning genes from the rest of the multicellularity functionalities (including

Figure 1. Expression Changes in the tRNA Pool in Proliferation, Differentiation, and Senescence

(A) A sample of correlation plots depicting similarity between tRNA abundance measurements (log scale) obtained with the microarrays on one hand and the extent of the transcription activation-associated H3K27ac modification as measured in ENCODE on the other. Each dot represents a tRNA type (all tRNA genes with same anticodon are grouped; a total of 206 tRNA genes, which are covered both on the array and in ENCODE, are represented).

(B) An expression matrix of the tRNAs in DLBCL and normal B cells. Each horizontal line represents a biological sample: upper 68 lines are DLBCL samples, and bottom 10 lines are normal B cells; each column represents a tRNA type, grouped by anticodon. The expression values in all 10 normal samples were averaged, and the color code depicts (log2) fold-change of each tRNA type (averaged over all iso-acceptor groups) in each sample relative to the average of the 10 normal samples.

(C) Hierarchical clustering of all sample types based on changes in tRNA expression profiles. Each column and row represents the average of all samples belonging to the same type, where the numbers in parentheses denote the number of samples belonging to that type. Off-diagonal entries denote the Pearson correlation between the tRNA expression profiles of two different sample types. The main diagonal, from top right to bottom left, depicts the median Pearson correlation among all pairs of samples within a given type of samples.

(D) A sample of correlation plots depicting similarity between changes in the tRNA pool among different types of proliferative and differentiated/arrested samples. Each dot represents a tRNA type.

(E) A PCA in which biological samples are represented in the space of tRNA pool expression changes; all points represent an average over three biological replicates. Neighboring dots represent pairs of samples in which the expression of the tRNA pool changes similarly. Three time-course treatments are shown: the red arrows depict the change in the tRNA pool during release from serum starvation, one of the blue arrows represents the change in the pool during differentiation of stem cells (time points are marked by blue triangles), and the second upon induction of senescence (time points are marked by blue circles).

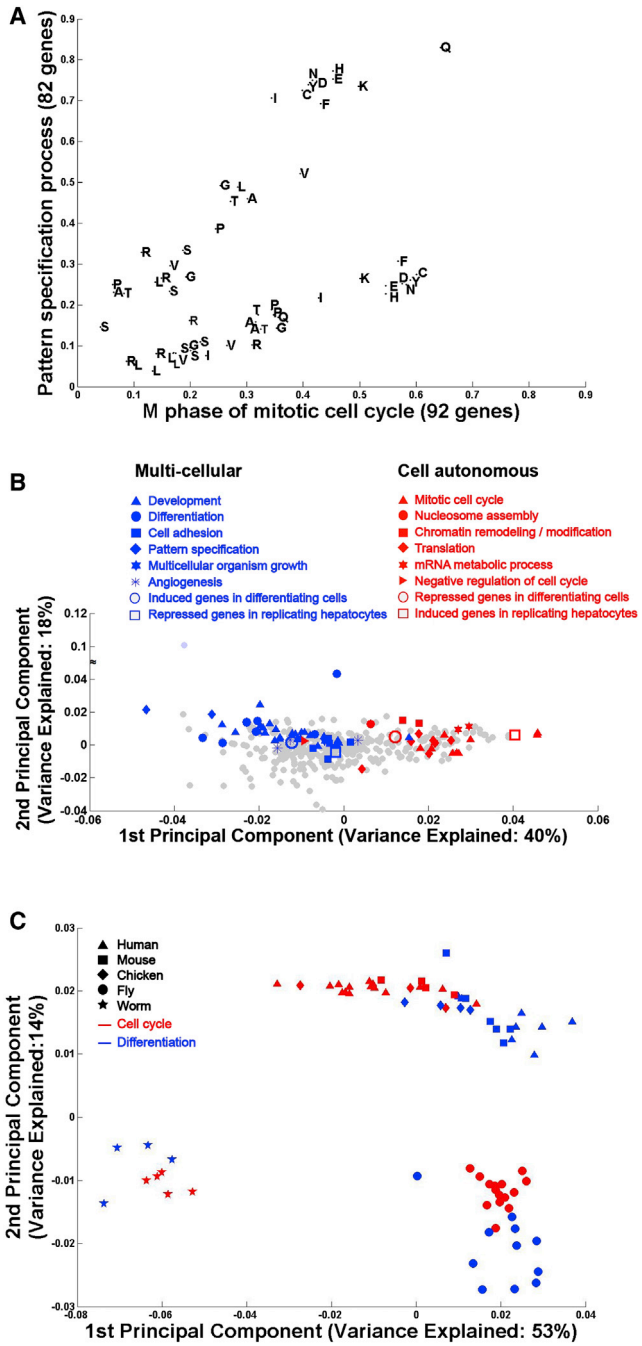

Figure 2. Codon Usage of Various Functional Gene Categories

(A) A dot plot depicting amino acid-normalized codon usage in two functional gene sets, "M phase of the mitotic cell cycle" and "pattern specification." Each dot represents one codon of the genetic code, represented by the corresponding amino acid. The value of a codon on the x axis is the probability that the codon will be used given that its encoded amino acid is used in cell-cycle genes, whereas the values on the y axis depict the probability of using the codon given the amino acid in patterning specification genes.

(B) A PCA projection of the human codon usage. Most gene sets (filled symbols) are derived from the GO; sets indicated by empty symbols are derived from expression data. The location of each gene set in this space is determined by the average codon usage of all the genes that belong to it. The % variance, out of the total original variance in the high-dimensional space, spanned by the first and second PCs is indicated on the x and y axis, respectively.

(C) Similarity in codon usage of the cell cycle and differentiation genes in five animals. We pooled together from each of the five species the genes belonging to each of the two GO categories and ran the analysis on all ten gene sets together.

cell adhesion, immune response, signal transduction, and stress response; Figure S2B). This indicates a slight, yet consistent difference in codon usage between these types of function.

To complement the GO-based classification, we also examined an annotation-independent classification of genes that is solely based on expression measurements of proliferating or differentiating/differentiated cells. The first paradigm was that of dividing versus differentiated hepatocytes. In a recent study, dividing liver cells were identified and isolated from the mature organ, and transcriptome analysis indicated that they undergo dedifferentiation (Klochendler et al., 2012). In particular, the study designated genes that are either induced or repressed in the dividing liver cells compared to the rest of the differentiated organ. We examined each of these gene sets and found that the proliferation-induced genes and the proliferation-repressed genes have a clear distinction in their codon usage (Figures 2B and S2C). Conversely, examining stem cells at the 5th day after induction of differentiation, we found that differentiation-induced and differentiation-repressed genes can be distinguished by their codon usage, with differentiation-repressed genes showing an overall higher similarity to the codon usage of the cell-cycle genes (Figures 2B and S2C).

Importantly, we observed a similar distinction in the codon usage of the proliferation genes and the differentiation genes in other vertebrates too, including mouse and chicken, indicating that this distinction in codon usage of the two programs is deeply rooted in vertebrate evolution. This is shown in Figure 2C, which was obtained after pooling together the genes from the two GO categories "cell cycle" and "cell differentiation" from the above vertebrates, in addition to the fly and the worm, and projecting all 10 gene sets on a PCA plane. Interestingly, the fly also shows the distinction in codon usage, yet the actual codons enriched in proliferation and in differentiation in this organism are distinct from the codons that are preferentially used to encode these programs in the vertebras. This indicates that vertebrates and insects may have converged independently toward separation in codon usage of proliferation and differentiation genes, albeit with different codons realizing this separation. In contrast, the worm *Caenorhabditis elegans* does not show a separation in codon usage between proliferation and differentiation genes, perhaps consistent with the fact that the fate acquisition in this species happens through mitotic cell division (Sulston and Horvitz, 1977) (Figures 2C and S2D). Rather than a separation between proliferation and differentiation genes, the main distinction in codon usage in the worm (that corresponds to the first PC) is between genes with high and low translation-efficiency levels (Figure S2E, right panel). Interestingly, in humans, separation of GO categories according to expression level (by translation-efficiency measure) is obtained too, but only in the third PC, which by definition spans less of the variance in the data (Figure S2E, left panel).

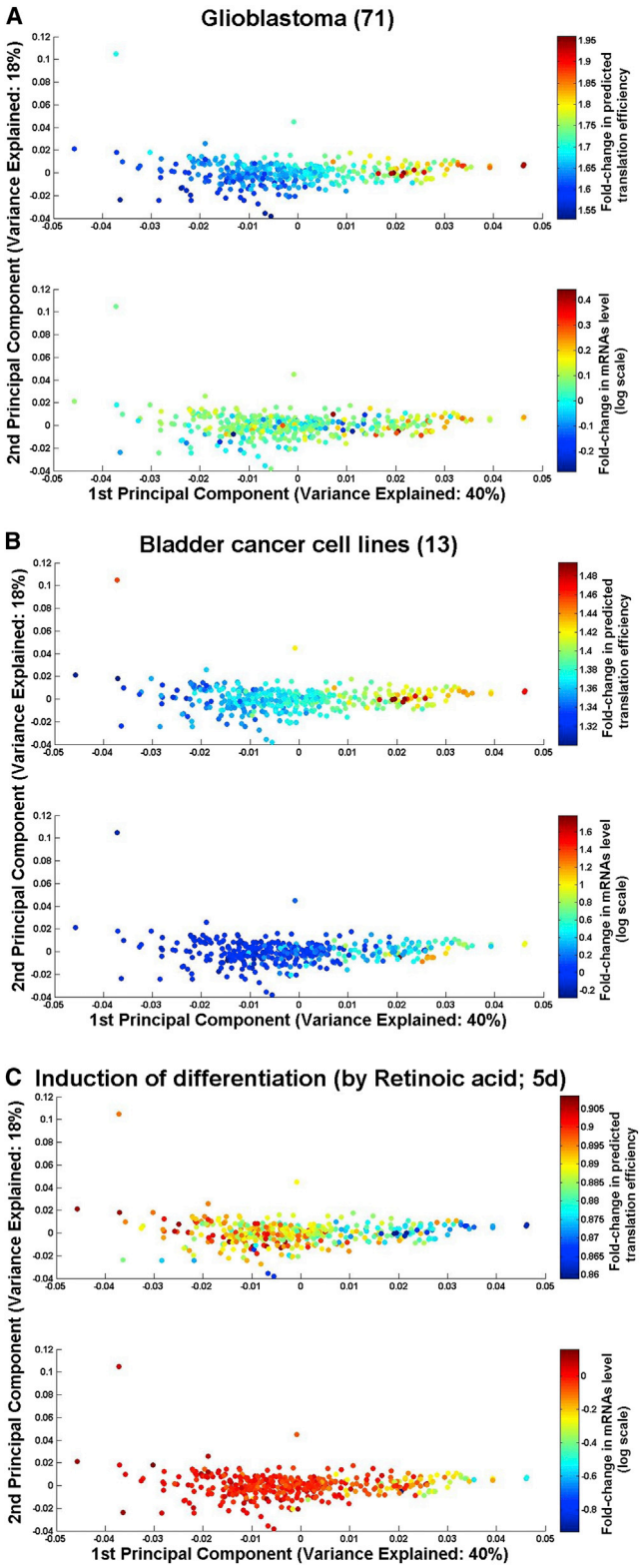

Figure 3. Projection of the tRNA and mRNA Expression Changes on the Codon-Usage Map

The same PCA map for codon usage as in Figure 2B is drawn, with overlay, by a color code, representing the expression change of tRNAs and mRNAs (upper and lower panels in each subplot, respectively) in proliferation and differentiation. Upper panel in each subplot: each gene category is color coded according to the relative change in availability of the tRNAs that correspond to the codon usage of its constituent genes, averaged over all genes in the category; the variation in the tRNA availability of each individual gene was calculated by the weighted arithmetic average of the fold-changes in the expression of the tRNA iso-acceptors that serve in translating it. Thus a red color for a given gene category indicates that on average the genes in that category have codons that mainly correspond to the tRNAs that are induced in the condition, whereas a blue color indicates that the codon usage in the categories is biased toward the tRNAs that were repressed in that given condition. The lower panel in each subplot displays changes at the mRNA level, averaged over all the genes in each gene category under the same conditions as in the upper panel, where here too red means that the genes were induced under the mentioned condition. In (A) and (B), the conditions are cancerous cells (glioblastoma primary cancer and bladder cancer cell lines; additional conditions in Figure S3), whereas in (C), the condition is induction of stem cells to differentiation by retinoic acid (day 5 after treatment).

Proliferation Genes Preferentially Use Codons Matching tRNAs Upregulated in Proliferating Cells

So far, we have shown that the tRNAs and the codon usage have distinct signatures in proliferation and differentiation, but do the anticodons carried by the proliferation-induced tRNAs show a bias toward the codons that are enriched in the proliferation genes? Indeed, we found that the cancer-induced tRNAs typically correspond, either perfectly or via wobbling, to codons enriched among the proliferation-processes genes. To visualize these results, we calculated the expected translational efficiency for the genes in each GO category based on their codon sequence and the cancerous versus the normal tRNA pool (Figures 3A, 3B, and S3A–S3D, upper panels). In parallel, we examined the changes at the mRNA levels of various gene sets (Figures 3A, 3B, and S3A–S3D, lower panels). It is well known that the proliferation- and gene expression-related genes are induced in cancer, and that differentiation genes are often repressed in cancer (Kumar et al., 2012). We found that cancer-induced mRNAs have distinct codon usage as they are clustered in the codon-usage space away from the cancer-repressed genes (Figures 3A, 3B, and S3A–S3D, lower panels).

Conversely to cancer, when we examined the tRNA pool at the 5th day after induction of differentiation of stem cells with retinoic acid, we found that the induced tRNAs largely correspond to the codons that are enriched among the multicellularity side of the codon-usage map, which again correlates well with the changes in mRNA expression levels (Figure 3C). Hence, in both cancer and differentiation, we can clearly observe a good correspondence between supply and demand: induction of genes at the mRNA level is typically accompanied by induction of the tRNAs needed for their translation (Figures 3A–3C and S3A–S3D, and see also Figure S3E).

Histone Modifications and tRNA Regulatory Elements Reflect Coordination between Expression of tRNA Types and mRNA Clients

The correlation between changes at the mRNA and tRNA levels suggests the existence of coordination between supply and demand in translation. To investigate such coordination further, we inspected the histone modification patterns in the vicinity of tRNA and mRNA genes in the human genome, given that RNA

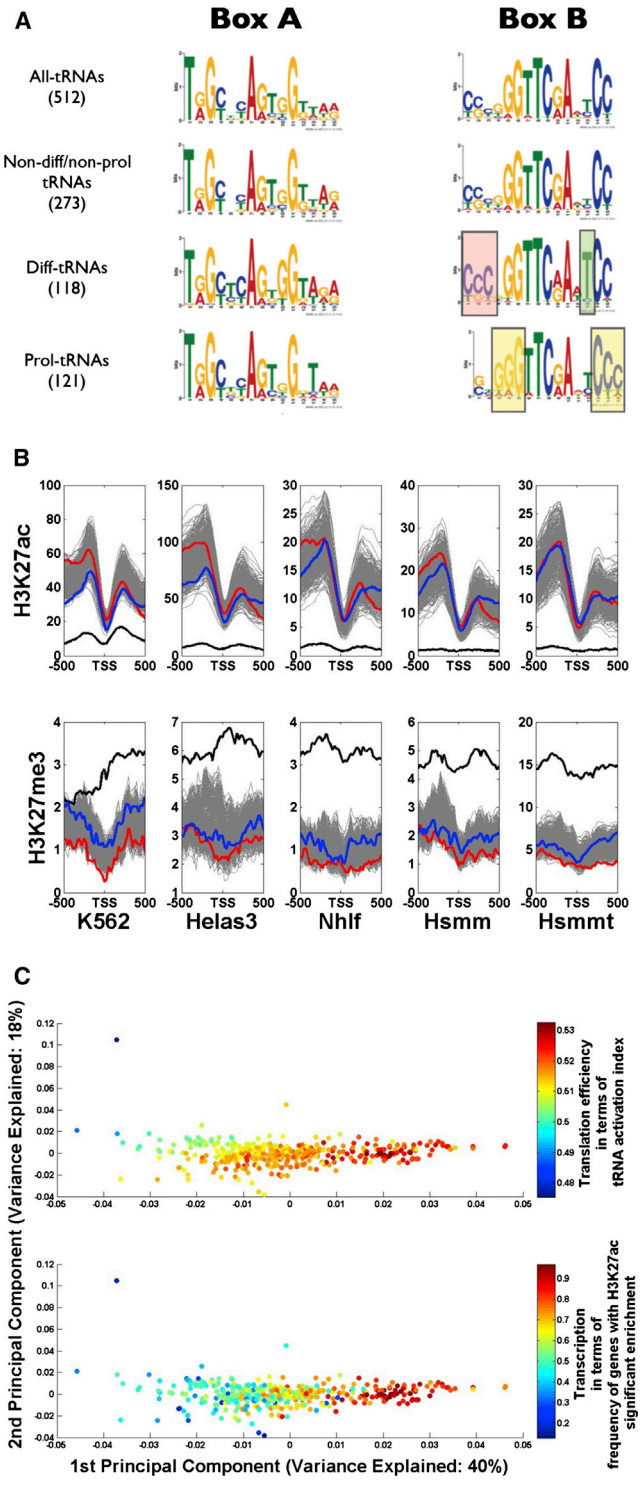

Figure 4. Histone Modification Coordination between tRNA Supply and Demand

(A) Sequence logo of the box A and box B in the promoters of all tRNA genes, in the tRNAs that are neither proliferation nor differentiation associated, in the differentiation tRNAs, and in the proliferation tRNAs. The positions that are most distinctive between the proliferation and differentiation tRNAs' versions of the motifs are highlighted.

(B) Density profiles of H3K27ac and H3K27me3 modifications in the vicinity of tRNA genes in either proliferating (cancerous) or differentiated mature cells. All tRNA genes are aligned according to their TSSs, and the regions of 500 bp upstream and downstream of the TSS are shown on the x axis. The y axis shows the averaged density of these two modifications as a function of distance from the TSS. Shown are the signals (y axis) of the following gene sets: tRNAs that are not occupied by RNA Pol III (colored in black); occupied "pro-proliferation" tRNAs (75 genes, colored in red); and occupied "pro-differentiation" tRNAs (81 genes, colored in blue). Each gray line is an average of a random set of 81 tRNA genes, sampled from 299 occupied human tRNA genes. p value analysis on the difference between the proliferation and differentiation tRNAs is in Figure S4E. Occupancy data were retrieved from Oler et al. (2010).

(C) The codon-usage PCA map as in Figures 2 and 3, colored here according to the density of the activating modification H3K27Ac in the vicinity of tRNA genes (upper panel, see details in the Experimental Procedures section) or in vicinity of mRNA-coding genes.

Pol III and RNA Pol II share similar modifications associated with either transcriptional activation or repression (Barski et al., 2010; Oler et al., 2010).

We first found that usage of a codon tends to correlate with the extent of histone modification around tRNA genes with the corresponding anticodon (Figure S4A illustrating H3K27ac). Focusing on the "cell cycle" and "cell differentiation" gene categories, we defined two sets of tRNAs: one holding tRNAs corresponding to codons over-represented among the cell-cycle genes and another with tRNAs corresponding to codons over-represented among the cell-differentiation genes (listed in Table S2). We called the two sets "proliferation tRNAs" and "differentiation tRNAs," respectively. To examine whether this classification corresponds to the transcriptional regulation of the tRNA genes, we analyzed their promoter sequences and epigenetic histone modifications. The promoter in tRNA genes is internal and consists of two known motifs, the "box A" and the "box B." To search for sequence differences, we ran a motif-finding algorithm (MEME, see Experimental Procedures) separately on the 121 proliferation tRNA genes and on the 118 differentiation tRNA genes. Remarkably, we found that especially the box B significantly differs between tRNAs involved in proliferation or differentiation, indicating distinct and concerted regulation of their transcription (Figures 4A and S4B).

We next used the ENCODE data to inspect the chromatin state around the upstream and downstream regions of the tRNA genes from the two sets and at the flanking regions of the corresponding protein-coding genes from each of the "cell cycle" and "cell differentiation" GO categories. Figures 4B and S4C show the tRNA and mRNA level analysis, respectively. In both figures, we depict the density of the selected activation-associated modification (H3K27ac) and the repressing modification (H3K27me3) in two cancer cell lines and three differentiated normal cell lines (Figures 4B and S4C; see also Figure S4D for additional chromatin modifications and Figures S4E and S4F for statistical significance analysis). We made several observations: (1) when examining the activation-associated modification, the upstream regions of the proliferation tRNAs were more heavily modified than their differentiation counterparts, predominantly in the cancer cells, (2) the repressing modification, H3K27me3, shows the opposite behavior, consistent with lower transcription rate of the differentiation tRNAs in all samples, (3) in the

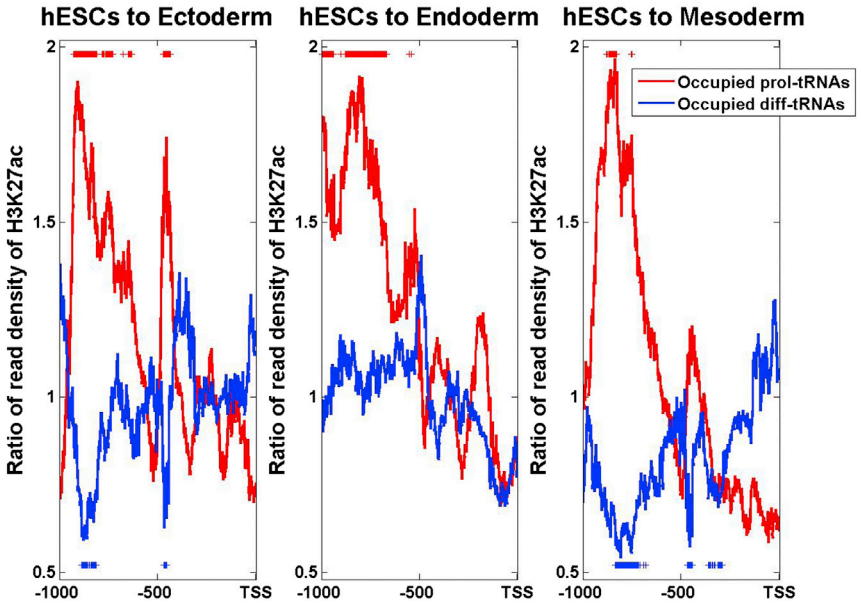

Figure 5. Change in Histone Modification around the Genomic Locations of tRNAs in Differentiation

The average level of H3K27Ac in the genomic vicinity of all proliferation (red) and differentiation (blue) tRNAs is depicted as a ratio between hESCs and cells differentiated from the stem cells into ectoderm, endoderm, and mesoderm. The transcription start site is marked with TSS. A randomization test (see Experimental Procedures) was devised that assesses the significance of the deviation of the proliferation tRNAs above the value of 1, and the differentiation tRNA below 1 at any given position around the TSS. Whenever the test for either tRNA set had a p value < 0.05, a "+" was marked in red and blue, respectively.

differentiated cells, the gap in activation modifications of the two tRNA sets was much more narrow and even closed in some cases, and (4) these changes around the tRNA genes are largely mirrored at the levels of the corresponding proliferation and differentiation protein-coding genes, which also show a higher extent of activation modifications for the proliferation genes compared to the differentiation genes, and a reversed trend for the repressing modification (Figure S4C). Note, however, that the dynamic activity is also seen upstream to the transcription start site (TSS), whereas the classical view of the tRNA promoter is that it is located downstream from the TSS (Galli et al., 1981). It is thus possible that potentially functional information as to the transcriptional control of tRNA exists also upstream to the TSS.

Next, we colored all the gene categories in the codon-usage PCA map, this time according to the information on the H3K27ac activation-associated chromatin modification (Figure 4C) around either the corresponding tRNA genes (upper panel) or the mRNA-coding genes themselves (lower panel). Shown here is the case of the K562 leukemia cell line. We found that the genes on the cell-autonomous (right) side of the map have codons that strongly correspond to the tRNAs that are associated with the activating modification, whereas the genes on the multicellularity (left) side of the map show the opposite behavior. Here the coordination with the mRNA level is clearly seen as well. The protein-coding genes on the cell-autonomous side of the codon-usage map are more often associated with activating modifications compared to the genes on the multicellularity side of the map.

Histone Modifications around the tRNA Genes Change Dynamically during Cellular Differentiation and Cancerous Transformation

To systematically examine the notion of dynamic changes of histone modifications in the vicinity of tRNA genes during differentiation and cancer, we inspected histone modifications in two available data sets: the first when hESCs were differentiated into the three germ layers (Gifford et al., 2013), and the second in cancer versus normal cells. When ESCs were differentiated into either ectoderm, endoderm, or mesoderm, we consistently observed a significant (p value < 0.05) reduction in H3K27ac on the proliferation tRNA genes and, correspondingly, higher levels of modifications on the differentiation tRNA genes in each of the three germ layers (Figure 5A). This indicates that each of the three differentiation treatments shows a dynamic reduction in activation of the proliferation tRNAs and a shift toward expressing the differentiation tRNAs. Similarly, we noticed a modest trend in which the cell-autonomous gene sets are consistently less intensely modified with H3K27Ac in differentiated skeletal muscle myotube (HSMMtube) compared to its less differentiated precursor (HSMM) (Bernstein et al., 2012), whereas GO categories associated with multicellularity show the opposite behavior (Figure S5A). Inspecting cancerous transformation of normal prostate cells (Bert et al., 2013), similar to one of the conditions tested on our above-mentioned array platform, we examined data on the reciprocal, repression-associated modification, H3K27me3. As expected, we found that the amount of this repressive modification increases on the differentiation tRNAs in cancer, whereas the modification of the proliferation tRNA set is somewhat reduced (Figure S5B).

DISCUSSION

We here describe the existence of function-related translational codes hardwired into the genetic code. The regulation of the tRNAs, which constitute the proliferation and differentiation programs, appears to work in concert with other gene-expression programs operating in the cell, so that coordinated changes occur at the mRNA level and at the tRNA level. Particularly, we found that changes at the mRNA level in proliferating or differentiated cells are coordinated with corresponding changes at the tRNA availability level. These observations thus demonstrate coordination between tRNA supply and demand. This coordination may manifests a general design principle in gene expression: the entire process appears to be coupled across its multiple stages

(Dahan et al., 2011; Lotan et al., 2005, 2007). The tRNA availability is known to be regulated at various levels including transcription, posttranscriptional processing, amino acid loading, and degradation. Although each level could make important contributions, here we have used comprehensive transcriptomic and epigenomic mapping to suggest a substantial role for the transcriptional level.

Why do cells coordinate supply and demand in translation? The observed coordination might be essential as a means to ensure high expression of certain genes, i.e., genes that are highly expressed at the mRNA level at a certain cellular state might also be translated more efficiently due to their good adaptation to the tRNA pool at that state. An alternative consideration does not implicate the matching between supply and demand in expression of particular genes but would rather suggest that proper coordination between supply and demand may allow optimization of the overall translation-resource allocation in the cell. According to this notion, when supply and demand are balanced, ribosomes are expected to flow with little congestion, and hence production costs are minimized.

Some studies found no evidence for translational selection in human (dos Reis et al., 2004; Kanaya et al., 2001), suggesting that synonymous codons in human are not selected to maximize translation efficiency (Lercher et al., 2003). Conversely, other studies do indicate weak, yet significant, translational selection in human, according to estimates of codon-usage adaptation to the global tRNA pool (Comeron, 2004; Lavner and Kotlar, 2005), and in vertebrates more generally (Doherty and McInerney, 2013). The conservation of the dual translational programs among the vertebrates examined here shows that this is not a human-specific trait but rather a much more ancient one that could have been selected for over prolonged evolutionary periods and large population sizes.

Why did the translation system evolve to operate with two distinct modes in proliferation and differentiation? We speculate that the separation into a dual program can "lock" the differentiated cells in a stable state that prevents undesired proliferation and transformation. According to this model, if, due to noisy transcriptional leakage, a given pro-proliferation gene was abnormally expressed in the cell, it would not be translated efficiently because the tRNA pool is relatively devoid of tRNAs that correspond to its codon usage. In this respect, the presence of distinct translational programs may serve to reduce aberrant expression resulting from transcriptional or posttranscriptional noise and ensure stable cell-fate decisions during processes such as differentiation. As such, the existence of a dual translational program may serve to "canalize" cellular processes (Waddington, 1942) and might thus initially serve as a cancer-protective mechanism. However, such a translation program may also act as a double-edged sword because, if cancer hijacks this program by selectively upregulating proliferative tRNAs, it will have the potential to boost the translation of pro-cancerous transcripts.

EXPERIMENTAL PROCEDURES

Sample Preparation

This study comprised human tissue (cancer and normal) samples from patients and healthy donors as well as a range of cell-based model systems depicted in Table 1. All the information about sample collection and preparation is available in Extended Experimental Procedures and Table S4.

Data Sources

Expression Profiling of Human tRNAs and mRNAs in Different Cancerous Cell Types and Physiological Conditions

Expression profiles were measured using custom-made microarrays (Nimblegen). The microarrays contain probes for 6,856 protein-coding transcripts and 26,910 ncRNAs including 294 probes corresponding to 206 tRNA genes. The various cell types from which RNA was hybridized onto the array are detailed in Table 1. Our microarray platform was recently shown to be useful for characterization of known and also putative human transcripts and was shown to largely agree with RNA sequencing data, especially among genes that are as highly expressed (Nielsen et al., 2014). Detailed information about the array design appears in Supplemental File S2.

tRNA Gene Copy Number

The tRNA gene copy numbers of all analyzed species were downloaded from the Genomic tRNA Database (http://lowelab.ucsc.edu/GtRNAdb/) (Lowe and Eddy, 1997).

Coding Sequences

The coding sequences of *H. sapiens* and *M. musculus* were downloaded from the Consensus CDS (CCDS) project (ftp://ftp.ncbi.nlm.nih.gov/pub/CCDS/). The coding sequences of *C. elegans* were downloaded from Ensembl ftp site (http://www.ensembl.org) (WS210, release 59). The coding sequences of *D. melanogaster* were downloaded from FlyBase (http://flybase.org/).

Classification of Gene Categories

Defined gene categories by biological process were downloaded from the Gene Ontology project (http://www.geneontology.org/); to avoid too-small gene sets, we only considered those with at least 40 genes.

Chromatin Modification

Fragment densities for 25 bp bins along the genome and discrete intervals of ChIP-seq fragment enrichment were downloaded from the Broad Histone (wgEncodeBroadHistone) Track at UCSC website (http://genome.ucsc.edu/).

Calculation of the Variation in the Human tRNA Pool

For each tRNA type (i.e., anticodon) in a given sample, we summed the expression of its corresponding individual genes. Then we divided the expression of each tRNA type by its averaged expression in either normal cells of the same tissue (for primary tumors and cancerous cell lines) or the corresponding reference condition (e.g., for cells released from starvation, the reference was starved cells; for cells induced to proliferate by overexpresion of an oncogene, the reference was cells transduced with an empty vector, etc.) (see Table 1 for a detailed description). Finally, for a given cell type, we averaged the fold-changes in the tRNA expression across all of its corresponding samples, e.g., over 68 samples for DLBCL (see in Table 1).

Estimating Translational Efficiency in Terms of tRNA Activation Index

We generated a new measure of translational efficiency (implemented in Figure 4C), termed henceforth as "tRNA activation index" (tACI). Our measure is calculated similarly to the tAI measure of translation efficiency (dos Reis et al., 2004), with one major change—we determine tRNA availability in terms of chromatin modification enrichment rather than gene copy numbers. As such, the new measure can be computed for every condition in which chromatin data exist.

Employing the aforementioned discrete intervals of ChIP-seq fragment enrichment, we set the activation score of each individual tRNA gene to be the average enrichment of the activating H3K27ac modification overlapping the 1,000 bp centered around its TSSs. Individual tRNA genes, for which no statistically significant signal enrichment was found, were classified as "not activated." Next, we defined the activation score of each tRNA type (anticodon) by the sum of the activation scores of its gene copies. Then, we determined the translation efficiency of an individual codon by the extent of activation of the tRNAs that serve in translating it, incorporating both the fully matched tRNA as well as tRNAs that contribute to translation through wobble rules (Crick, 1966).

Formally, the translation efficiency score for the *i*–th codon is as follows:

$$W_i = \sum_{j=1}^{n_i} (1 - s_{ij}) tCME_{ij},$$

where *n* is the number of tRNA isoacceptors that recognize the *i*-th codon, $tCME_{ij}$ denotes the sum of the chromatin *m*odification enrichment (CME) of the activated copies of the *j*-th tRNA that recognizes the *i*-th codon, and s_{ij} correspond to the wobble interaction, or selective constraint on the efficiency of the pairing between codon *i* and anticodon *j*, as was determined and implemented for the original tAI measure. As done in the original tAI formalism by dos Reis et al., the scores of the 61 codons are further divided by the maximal score, and finally, the tACI value of a gene with L codons is then simply calculated as the geometric mean of the w_i's of its codons:

$$tACI(g) = \sqrt[L]{\prod_{c=1}^{L} w_c}$$

Motif Finding

The box A and B motifs, the promoter motifs within tRNA genes, were predicted using the motif discovery algorithm MEME (v4.6.1; Bailey and Elkan, 1994) with the following parameters: -dna -mod zoops -nmotifs 2 -minw 15 -maxw 15. Box A and B motifs were learned separately for all (512), unclassified (273), differentiation (118), and proliferation (120) tRNA genes. Differences in box A and B motifs between tRNA sets were assessed using a Pearson correlation-based motif similarity score (Pietrokovski, 1996). The score was maximized over all ungapped motif alignments and normalized by the average motif length. Differences between motifs were assessed using a permutation test in which the observed motif similarity score was compared against a set of 1,000 permutation-based motif similarity scores. Permutation samples were obtained by randomly sampling tRNA genes from the whole pool of tRNA genes while considering the observed tRNA sample set sizes. Motifs were considered to be significantly different if the observed motif similarity score was within 1% of the lowest permutation-based similarity scores (i.e., one-tailed p value of 0.01).

Assessing the Significance of Dynamic Changes of Histone Modifications in tRNA Genes' Vicinity during Proliferation and Differentiation

For each experiment, we first normalized the read density of either the H3K27ac (Figure 5) or H3K27me3 (Figure S5B) histone modification, to achieve overlapping distribution of either the proliferating or differentiating cell types and their precursor. For each cell type of a given experiment, we then sampled 500 times two random tRNA gene sets, where one of the sets had a set size equal to that of the proliferation tRNAs, and the other of the differentiation tRNAs. Next, we averaged the histone modification density for the members of each random set and computed either the ratio between the averages of each cell type to that of its precursor or the ratio between the averages of the precursor and its derived cell types at each position along the sequence coordinates. p values were calculated at each sequence position as (1) the fraction out of 500 random samples that showed higher ratios compared to the examined ratio—for either the ratio seen between the proliferation tRNAs in hESC compared to ectoderm/mesoderm/endoderm or the differentiation tRNAs in prostate cancer compared to normal cells; (2) the fraction out of 500 random samples that showed lower ratios compared to the examined ratio—for either the ratio seen between the differentiation tRNAs in hESC compared to ectoderm/mesoderm/endoderm or the proliferation tRNAs in prostate cancer compared to normal cells.

SUPPLEMENTAL INFORMATION

Supplemental Information includes Extended Experimental Procedures, five figures, and four tables and can be found with this article online at http://dx.doi.org/10.1016/j.cell.2014.08.011.

AUTHOR CONTRIBUTIONS

H.G., D.T., A.H.L., and Y.P. conceived the project, designed the work, analyzed all data, and wrote the paper. H.G. did the majority of the computational work; D.T. did the majority of the experimental work.

ACKNOWLEDGMENTS

Work in the authors' laboratory is supported by a European Research Council (ERC) grant (Y.P.) and by the Danish National Advanced Technology Foundation, the Danish Council for Strategic Research, the Danish Council for Independent Research, the Novo Nordisk Foundation, the Lundbeck Foundation, and the Danish Cancer Society (A.H.L.). Y.P. is an incumbent of the Ben-May Professorial Chair. S.M.K. was supported by a postdoctoral fellowship from the Netherlands Organisation for scientific research (NWO). The Centre for Epigenetics is supported by the Danish National Research Foundation (DNRF82). We thank Simon Kasif and Erez Dekel for stimulating discussions.

Received: December 25, 2013
Revised: May 13, 2014
Accepted: August 8, 2014
Published: September 11, 2014

REFERENCES

Almondes, K.G., Leal, G.V., Cozzolino, S.M., Philippi, S.T., and Rondó, P.H. (2010). The role of selenoproteins in cancer. Rev. Assoc. Med. Bras. *56*, 484–488.

Ashburner, M., Ball, C.A., Blake, J.A., Botstein, D., Butler, H., Cherry, J.M., Davis, A.P., Dolinski, K., Dwight, S.S., Eppig, J.T., et al.; The Gene Ontology Consortium (2000). Gene ontology: tool for the unification of biology. Nat. Genet. *25*, 25–29.

Bailey, T.L., and Elkan, C. (1994). Fitting a mixture model by expectation maximization to discover motifs in biopolymers. Proc. Int. Conf. Intell. Syst. Mol. Biol. *2*, 28–36.

Barski, A., Chepelev, I., Liko, D., Cuddapah, S., Fleming, A.B., Birch, J., Cui, K., White, R.J., and Zhao, K. (2010). Pol II and its associated epigenetic marks are present at Pol III-transcribed noncoding RNA genes. Nat. Struct. Mol. Biol. *17*, 629–634.

Bernstein, B.E., Birney, E., Dunham, I., Green, E.D., Gunter, C., and Snyder, M.; ENCODE Project Consortium (2012). An integrated encyclopedia of DNA elements in the human genome. Nature *489*, 57–74.

Bert, S.A., Robinson, M.D., Strbenac, D., Statham, A.L., Song, J.Z., Hulf, T., Sutherland, R.L., Coolen, M.W., Stirzaker, C., and Clark, S.J. (2013). Regional activation of the cancer genome by long-range epigenetic remodeling. Cancer Cell *23*, 9–22.

Comeron, J.M. (2004). Selective and mutational patterns associated with gene expression in humans: influences on synonymous composition and intron presence. Genetics *167*, 1293–1304.

Crick, F.H. (1966). Codon—anticodon pairing: the wobble hypothesis. J. Mol. Biol. *19*, 548–555.

Dahan, O., Gingold, H., and Pilpel, Y. (2011). Regulatory mechanisms and networks couple the different phases of gene expression. Trends Genet. *27*, 316–322.

Doherty, A., and McInerney, J.O. (2013). Translational selection frequently overcomes genetic drift in shaping synonymous codon usage patterns in vertebrates. Mol. Biol. Evol. *30*, 2263–2267.

dos Reis, M., Savva, R., and Wernisch, L. (2004). Solving the riddle of codon usage preferences: a test for translational selection. Nucleic Acids Res. *32*, 5036–5044.

Dutkowski, J., and Ideker, T. (2011). Protein networks as logic functions in development and cancer. PLoS Comput. Biol. *7*, e1002180.

Galli, G., Hofstetter, H., and Birnstiel, M.L. (1981). Two conserved sequence blocks within eukaryotic tRNA genes are major promoter elements. Nature *294*, 626–631.

Gifford, C.A., Ziller, M.J., Gu, H., Trapnell, C., Donaghey, J., Tsankov, A., Shalek, A.K., Kelley, D.R., Shishkin, A.A., Issner, R., et al. (2013). Transcriptional and epigenetic dynamics during specification of human embryonic stem cells. Cell *153*, 1149–1163.

Gingold, H., and Pilpel, Y. (2011). Determinants of translation efficiency and accuracy. Mol. Syst. Biol. *7*, 481.

Gingold, H., Dahan, O., and Pilpel, Y. (2012). Dynamic changes in translational efficiency are deduced from codon usage of the transcriptome. Nucleic Acids Res. *40*, 10053–10063.

Goodman, D.B., Church, G.M., and Kosuri, S. (2013). Causes and effects of N-terminal codon bias in bacterial genes. Science *342*, 475–479.

Hanahan, D., and Weinberg, R.A. (2000). The hallmarks of cancer. Cell *100*, 57–70.

Hsieh, A.C., Liu, Y., Edlind, M.P., Ingolia, N.T., Janes, M.R., Sher, A., Shi, E.Y., Stumpf, C.R., Christensen, C., Bonham, M.J., et al. (2012). The translational landscape of mTOR signalling steers cancer initiation and metastasis. Nature *485*, 55–61.

Ingolia, N.T., Lareau, L.F., and Weissman, J.S. (2011). Ribosome profiling of mouse embryonic stem cells reveals the complexity and dynamics of mammalian proteomes. Cell *147*, 789–802.

Kanaya, S., Yamada, Y., Kinouchi, M., Kudo, Y., and Ikemura, T. (2001). Codon usage and tRNA genes in eukaryotes: correlation of codon usage diversity with translation efficiency and with CG-dinucleotide usage as assessed by multivariate analysis. J. Mol. Evol. *53*, 290–298.

Klochendler, A., Weinberg-Corem, N., Moran, M., Swisa, A., Pochet, N., Savova, V., Vikeså, J., Van de Peer, Y., Brandeis, M., Regev, A., et al. (2012). A transgenic mouse marking live replicating cells reveals in vivo transcriptional program of proliferation. Dev. Cell *23*, 681–690.

Kudla, G., Murray, A.W., Tollervey, D., and Plotkin, J.B. (2009). Coding-sequence determinants of gene expression in Escherichia coli. Science *324*, 255–258.

Kumar, S.M., Liu, S., Lu, H., Zhang, H., Zhang, P.J., Gimotty, P.A., Guerra, M., Guo, W., and Xu, X. (2012). Acquired cancer stem cell phenotypes through Oct4-mediated dedifferentiation. Oncogene *31*, 4898–4911.

Kutter, C., Brown, G.D., Gonçalves, A., Wilson, M.D., Watt, S., Brazma, A., White, R.J., and Odom, D.T. (2011). Pol III binding in six mammals shows conservation among amino acid isotypes despite divergence among tRNA genes. Nat. Genet. *43*, 948–955.

Lavner, Y., and Kotlar, D. (2005). Codon bias as a factor in regulating expression via translation rate in the human genome. Gene *345*, 127–138.

Lercher, M.J., Urrutia, A.O., Pavlícek, A., and Hurst, L.D. (2003). A unification of mosaic structures in the human genome. Hum. Mol. Genet. *12*, 2411–2415.

Lotan, R., Bar-On, V.G., Harel-Sharvit, L., Duek, L., Melamed, D., and Choder, M. (2005). The RNA polymerase II subunit Rpb4p mediates decay of a specific class of mRNAs. Genes Dev. *19*, 3004–3016.

Lotan, R., Goler-Baron, V., Duek, L., Haimovich, G., and Choder, M. (2007). The Rpb7p subunit of yeast RNA polymerase II plays roles in the two major cytoplasmic mRNA decay mechanisms. J. Cell Biol. *178*, 1133–1143.

Lowe, T.M., and Eddy, S.R. (1997). tRNAscan-SE: a program for improved detection of transfer RNA genes in genomic sequence. Nucleic Acids Res. *25*, 955–964.

Mamane, Y., Petroulakis, E., LeBacquer, O., and Sonenberg, N. (2006). mTOR, translation initiation and cancer. Oncogene *25*, 6416–6422.

Navon, S., and Pilpel, Y. (2011). The role of codon selection in regulation of translation efficiency deduced from synthetic libraries. Genome Biol. *12*, R12.

Nielsen, M.M., Tehler, D., Vang, S., Sudzina, F., Hedegaard, J., Nordentoft, I., Orntoft, T.F., Lund, A.H., and Pedersen, J.S. (2014). Identification of expressed and conserved human noncoding RNAs. RNA *20*, 236–251.

Oler, A.J., Alla, R.K., Roberts, D.N., Wong, A., Hollenhorst, P.C., Chandler, K.J., Cassiday, P.A., Nelson, C.A., Hagedorn, C.H., Graves, B.J., and Cairns, B.R. (2010). Human RNA polymerase III transcriptomes and relationships to Pol II promoter chromatin and enhancer-binding factors. Nat. Struct. Mol. Biol. *17*, 620–628.

Pavon-Eternod, M., Gomes, S., Geslain, R., Dai, Q., Rosner, M.R., and Pan, T. (2009). tRNA over-expression in breast cancer and functional consequences. Nucleic Acids Res. *37*, 7268–7280.

Pavon-Eternod, M., Gomes, S., Rosner, M.R., and Pan, T. (2013). Overexpression of initiator methionine tRNA leads to global reprogramming of tRNA expression and increased proliferation in human epithelial cells. RNA *19*, 461–466.

Perou, C.M., Sørlie, T., Eisen, M.B., van de Rijn, M., Jeffrey, S.S., Rees, C.A., Pollack, J.R., Ross, D.T., Johnsen, H., Akslen, L.A., et al. (2000). Molecular portraits of human breast tumours. Nature *406*, 747–752.

Pietrokovski, S. (1996). Searching databases of conserved sequence regions by aligning protein multiple-alignments. Nucleic Acids Res. *24*, 3836–3845.

Qian, W., Yang, J.R., Pearson, N.M., Maclean, C., and Zhang, J. (2012). Balanced codon usage optimizes eukaryotic translational efficiency. PLoS Genet. *8*, e1002603.

Raha, D., Wang, Z., Moqtaderi, Z., Wu, L., Zhong, G., Gerstein, M., Struhl, K., and Snyder, M. (2010). Close association of RNA polymerase II and many transcription factors with Pol III genes. Proc. Natl. Acad. Sci. USA *107*, 3639–3644.

Saxonov, S., Berg, P., and Brutlag, D.L. (2006). A genome-wide analysis of CpG dinucleotides in the human genome distinguishes two distinct classes of promoters. Proc. Natl. Acad. Sci. USA *103*, 1412–1417.

Sonenberg, N., and Hinnebusch, A.G. (2009). Regulation of translation initiation in eukaryotes: mechanisms and biological targets. Cell *136*, 731–745.

Subramaniam, A.R., Pan, T., and Cluzel, P. (2013). Environmental perturbations lift the degeneracy of the genetic code to regulate protein levels in bacteria. Proc. Natl. Acad. Sci. USA *110*, 2419–2424.

Sulston, J.E., and Horvitz, H.R. (1977). Post-embryonic cell lineages of the nematode, Caenorhabditis elegans. Dev. Biol. *56*, 110–156.

Tuller, T., Waldman, Y.Y., Kupiec, M., and Ruppin, E. (2010). Translation efficiency is determined by both codon bias and folding energy. Proc. Natl. Acad. Sci. USA *107*, 3645–3650.

Waddington, C.H. (1942). Canalization of development and the inheritance of acquired characters. Nature *150*, 563–565.

Xu, Y., Ma, P., Shah, P., Rokas, A., Liu, Y., and Johnson, C.H. (2013). Non-optimal codon usage is a mechanism to achieve circadian clock conditionality. Nature *495*, 116–120.

Yang, J.H., Shao, P., Zhou, H., Chen, Y.Q., and Qu, L.H. (2010). deepBase: a database for deeply annotating and mining deep sequencing data. Nucleic Acids Res. *38* (Database issue), D123–D130.

Zhou, M., Guo, J., Cha, J., Chae, M., Chen, S., Barral, J.M., Sachs, M.S., and Liu, Y. (2013). Non-optimal codon usage affects expression, structure and function of clock protein FRQ. Nature *495*, 111–115.